THE JOURNAL OF BIOLOGICAL CHEMISTRY VOL. 287, NO. 34, pp. 28852–28864, August 17, 2012

Metabolism of Vertebrate Amino Sugars with *N*-Glycolyl Groups

*MECHANISMS UNDERLYING GASTROINTESTINAL INCORPORATION OF THE NON-HUMAN SIALIC ACID XENO-AUTOANTIGEN N-GLYCOLYLNEURAMINIC ACID**

Received for publication, March 22, 2012, and in revised form, May 25, 2012 Published, JBC Papers in Press, June 12, 2012, DOI 10.1074/jbc.M112.364182

Kalyan Banda[‡1], **Christopher J. Gregg**[§1], **Renee Chow**[¶], **Nissi M. Varki**[¶], **and Ajit Varki**[‡§2]

From the Departments of [‡]*Medicine,* [§]*Cellular and Molecular Medicine, and* [¶]*Pathology, Glycobiology Research and Training Center, University of California San Diego, La Jolla, California 92093-0687*

Background: Prior work implicated the sialic acid Neu5Gc as a xeno-autoantigen in humans.
Results: Dietary Neu5Gc can be utilized by the murine gastrointestinal system and distributed for glycosylation in peripheral tissues.
Conclusion: Diets containing Neu5Gc can lead to human-like tissue incorporation.
Significance: Neu5Gc may be a dietary risk factor for progression of carcinomas, atherosclerosis, and immunologic diseases in humans.

Although *N*-acetyl groups are common in nature, *N*-glycolyl groups are rare. Mammals express two major sialic acids, *N*-acetylneuraminic acid and *N*-glycolylneuraminic acid (Neu5Gc). Although humans cannot produce Neu5Gc, it is detected in the epithelial lining of hollow organs, endothelial lining of the vasculature, fetal tissues, and carcinomas. This unexpected expression is hypothesized to result via metabolic incorporation of Neu5Gc from mammalian foods. This accumulation has relevance for diseases associated with such nutrients, via interaction with Neu5Gc-specific antibodies. Little is known about how ingested sialic acids in general and Neu5Gc in particular are metabolized in the gastrointestinal tract. We studied the gastrointestinal and systemic fate of Neu5Gc-containing glycoproteins (Neu5Gc-glycoproteins) or free Neu5Gc in the Neu5Gc-free *Cmah*$^{-/-}$ mouse model. Ingested free Neu5Gc showed rapid absorption into the circulation and urinary excretion. In contrast, ingestion of Neu5Gc-glycoproteins led to Neu5Gc incorporation into the small intestinal wall, appearance in circulation at a steady-state level for several hours, and metabolic incorporation into multiple peripheral tissue glycoproteins and glycolipids, thus conclusively proving that Neu5Gc can be metabolically incorporated from food. Feeding Neu5Gc-glycoproteins but not free Neu5Gc mimics the human condition, causing tissue incorporation into human-like sites in *Cmah*$^{-/-}$ fetal and adult tissues, as well as developing tumors. Thus, glycoproteins containing glycosidically linked Neu5Gc are the likely dietary source for human tissue accumulation, and not the free monosaccharide. This human-like model can be used to elucidate specific mechanisms of Neu5Gc delivery from the gut to tissues, as well as general mechanisms of metabolism of ingested sialic acids.

Sialic acids are acidic capping sugars on glycan chains, found on the cell surface and secreted glycoconjugates in animals of the Deuterostome lineage (vertebrates and so-called "higher" invertebrates (1–3)). The localization and ubiquity of sialic acids underscore their importance in mediating numerous cellular and extracellular interactions and their requirement for embryogenesis (4). The 9-carbon core structure of sialic acids can be extensively modified to fine-tune these interactions. For example, hydroxylation of the C5 *N*-acetyl group of CMP-*N*-acetylneuraminic acid (CMP-Neu5Ac)[3] is catalyzed by the enzyme cytidine monophosphate *N*-acetylneuraminic acid hydroxylase, which generates CMP-*N*-glycolylneuraminic acid (CMP-Neu5Gc) (5–11). These two nucleotide sugars donate Neu5Ac and Neu5Gc for sialylation as the major sialic acids expressed in most mammals. Our companion paper (12) provides a more detailed discussion regarding cytosolic pathways of sialic acid metabolism and the relevance to the intracellular fate of Neu5Gc.

Despite the ubiquity of Neu5Gc in most mammals, CMP-Neu5Ac hydroxylase is nonfunctional in all humans (13, 14) due to an *Alu*-mediated deletion of *CMAH* exon 6 (15), causing premature truncation of the open reading frame (14). Thus, humans cannot produce Neu5Gc, only Neu5Ac. Neu5Gc was also absent in human-like *Cmah*$^{-/-}$ mouse (16, 17), showing that there exists no alternative pathway for Neu5Gc biosynthesis in mammals.

Interestingly, intracellular sialic acid biosynthetic enzymes do not discriminate between Neu5Gc and Neu5Ac, and exoge-

* This work was supported in part by National Institutes of Health Grant R01GM32373. This work was also supported by a research grant from the Institut Mérieux. A. V. and N. M. V. are co-founders of and consultants for Sialix Inc., a biotech startup company interested in the practical implications of Neu5Gc uptake in humans.

[1] Both authors contributed equally to this work.

[2] To whom correspondence should be addressed: Glycobiology Research and Training Center, Depts. of Medicine and Cellular and Molecular Medicine, University of California San Diego, 9500 Gilman Dr., La Jolla, CA 92093-0687; Tel.: 858-534-2214; Fax: 858-534-5611; E-mail: a1varki@ucsd.edu.

[3] The abbreviations used are: Neu5Ac, *N*-acetylneuraminic acid; DMB, 1,2-diamino-4,5-methylenedioxybenzene; Neu5Gc, *N*-glycolylneuraminic acid; PSM, porcine submaxillary mucin; rcf, relative centrifugal force; PNGase, peptide:*N*-glycosidase.

nous Neu5Gc can exploit this metabolic "loophole" to be used for sialylation of human cells (18). This finding is important in light of classic claims for the presence of Neu5Gc in human carcinomas and fetal tissues (19) using anti-Neu5Gc antibodies generated in chickens (the avian lineage also appears deficient in Neu5Gc and thus can be immunized against the antigen) (20). More recently, histology of human tissues using an affinity-purified monospecific version of such an antibody (αNeu5Gc IgY) has demonstrated several human tissues where Neu5Gc is characteristically present, such as endothelial cells lining the micro- and macro-vasculature (21), carcinomas (22), placental tissues (23), and epithelial cells lining hollow organs (24, 25). Given that humans who eat red meats and other mammal-derived food products consume milligram quantities of Neu5Gc each day (24), it is reasonable to propose that the Neu5Gc detected in human tissues originates from dietary sources. Previous human volunteer studies showed that orally ingested free Neu5Gc might be incorporated into salivary mucins in small amounts (24). However, the efficiency on incorporation was poor, and nothing could be stated about incorporation into endothelia, epithelia, cancers, or fetuses.

Although human sialic acid biosynthetic enzymes do not clearly discriminate between Neu5Ac and Neu5Gc, the human humoral immune system does, and all humans tested have circulating Neu5Gc-specific immunoglobulin (Ig) at variable (sometime high) levels (24, 26–28). These antibodies are known to arise during the 1st year of life (29). Recent work has also explored the potential pathologic role of Neu5Gc in human carcinomas (22, 30), atherosclerosis (21), and susceptibility to an *Escherichia coli* shiga-like SubAB toxin (25, 31). These studies suggest that Neu5Gc is actively exacerbating these diseases, in most cases through interactions with circulating Neu5Gc-specific Ig (21, 22). Thus, there is a need to understand mechanisms underlying tissue incorporation of ingested Neu5Gc and to conclusively prove that dietary Neu5Gc can be accumulated in a manner mimicking human-like tissue distribution.

It is known that mammalian infants require dietary sialic acid supplementation for optimal brain development (32). Dietary sialic acid also improves memory formation, learning metrics, and brain sialic acid content in piglets (33) and rats (34). Moreover, evidence has shown that breast milk as opposed to formula is much richer in sialic acid content (35, 36) and that breastfed children develop higher IQ levels than formula-fed children (37).

Despite these observations, remarkably little is known about the fate of ingested sialic acids in mammals. Aside from a few observations of sialidase activity in intestinal fluids (38), the only published studies on this topic were performed by Nöhle and Schauer (39–41). They showed that although radioactive free sialic acid fed to mice and rats appeared largely intact in the urine (39, 40), label from radioactively sialylated mucin-type glycoproteins was absorbed more slowly. A portion of the radioactive sialic acids were also metabolized (presumably by lyases), as evinced by radioactive CO_2 expired by the animals (41). Beyond this, little else is known about the fate of ingested sialic acids in mammals.

In this study, we have used a Neu5Gc-deficient mouse with a human-like defect in *Cmah* as a model, where ingested Neu5Gc can be followed like a tracer in a Neu5Gc-free environment, using a polyclonal chicken Neu5Gc-specific IgY antibody (αNeu5Gc IgY), and by fluorescent tagging of free sialic acids with 1,2-diamino-4,5-methylenedioxybenzene dihydrochloride (DMB) for HPLC. These reagents play a prominent role in this work and deserve an introduction to help the reader understand their respective utilities. Neu5Gc-containing glycoproteins can be detected by αNeu5Gc IgY because the antibody recognizes Neu5Gc in α-conformation (Fig. 1*A*, *left column*). Although the glycosidic linkage that covalently links Neu5Gc to the underlying glycan holds Neu5Gc in the α-conformation, free Neu5Gc monosaccharide is primarily (~90%) in the β-conformation (Fig. 1*A*, *right column*). Conversely, DMB requires the α-keto acid moiety of sialic acid to react and form the fluorescent adduct that is monitored in HPLC. This keto acid moiety is not available when sialic acids are glycosidically linked. Thus, DMB will only react with free Neu5Gc monosaccharide and not with Neu5Gc-glycoproteins. Glycosidically linked sialic acids can be released from glycans using acid hydrolysis (2 M acetic acid at 80 °C for 3 h) (42) and are available for DMB labeling thereafter.

The $Cmah^{-/-}$ mouse and these reagents (Fig. 1*A*) allowed us to study the gastrointestinal kinetics of ingested Neu5Gc *in vivo*, the appearance of dietary metabolites in the blood and urine, and to ascertain the tissues where dietary Neu5Gc is metabolically incorporated *in vivo*. Given that Neu5Gc is thus far the only example of a foreign immunogenic molecule that is incorporated in human tissues and is likely responsible for exacerbating chronic inflammatory conditions, the study of its gastrointestinal kinetics and metabolic incorporation is of importance to human health and disease.

EXPERIMENTAL PROCEDURES

Mice and Chow—$Cmah^{-/-}$ mice have been described previously (16). Mice were housed in an Association for Assessment and Accreditation of Laboratory Animal Care-approved vivarium with 12-h diurnal lighting and access to food and water *ad libitum*. $Cmah^{-/-}$ mice were maintained on a Neu5Gc-deficient soy-based chow (Dyets, Inc.; 110951 for adults; 110751 for pregnancy/weaning) to ensure that animals were not exposed to Neu5Gc prior to experiments. We confirmed that this chow is free of Neu5Gc by DMB-HPLC and is also free of sialic acids by the thiobarbituric acid reaction (data not shown). The Institutional Animal Care and Use Committee at University of California San Diego, approved all researchers and animal procedures.

Other Reagents—All reagents and chemicals were purchased from Fisher or Sigma, unless otherwise specified.

Free Neu5Gc and Neu5Gc-glycoproteins for Feeding Studies—Free Neu5Gc was either purchased commercially (Inalco) or synthesized according to published methods (43). Porcine submaxillary mucin (44) was used as a source of mucin-type glycosidically linked Neu5Gc-containing glycoproteins (Neu5Gc-glycoproteins). Porcine submaxillary glands (Pel-Freez Biologicals) were finely chopped and homogenized in 5 volumes of water. Homogenates were centrifuged at 8000 rcf for 15 min, and the supernatant was then filtered through glass wool. The mucin was precipitated by gradual acidification (to pH 3.5)

at 4 °C, mixed overnight at 4 °C, and then left to settle. The supernatant was removed by siphoning, and the precipitated mucin was centrifuged at 400 rcf for 15 min, washed with water, and centrifuged again. Mucin pellets were neutralized to pH 8.0 and dialyzed using a 10,000 molecular weight cutoff CE membrane (Spectrum Labs) against 20 volumes of water, with at least 5 volume changes. This preparation, called porcine submaxillary mucin (PSM), was then dried by lyophilization, and its Neu5Gc content was characterized by DMB-HPLC.

PSM was chosen for this work because the only previous dietary feeding studies of sialic acid used a radioactively resialylated mucin (39, 40) and because it has very high Neu5Gc content (7–9% by weight). Also relevant to our decision was the practicality of producing large quantities needed for long term feeding studies and the minimal nutritional impact on the mouse diet (less than 1% by weight of the chow).

Neu5Gc-glycoprotein chow was generated by adding purified PSM to Neu5Gc-free chow, followed by autoclaving. Alternatively, purified PSM was provided to a manufacturer for incorporation into the chow prior to pelleting and sterilization by γ-irradiation. Neither autoclaving nor irradiation caused significant release of Neu5Gc from PSM. A Western blot of the chow was also run before and after sterilization and showed no change.

Short Term and Long Term Feeding of Neu5Gc—Cmah$^{-/-}$ mice were gavaged with 1 mg of Neu5Gc using gavage needles (Braintree Scientific). At the appropriate time after feeding, animals were anesthetized using isoflurane (VetOne), and blood was collected by cardiac puncture. Next, we made a ventral midline incision that exposed the peritoneal cavity and then isolated and cannulated the proximal duodenum on a blunt-end needle. The small intestine was secured to the needle using 6.0 silk sutures (Braintree Scientific). We then isolated and clamped the distal ileum at the ileocecal junction and detached the small intestine from the cecum. The entire small intestine was flushed out with 6 ml of PBS via cannulation, and the contents were collected from distal ileum into a glass conical tube. The contents of the small intestine were dried down and resuspended in 1 ml of H_2O. The small intestine (~30 cm) was then divided into three equal segments. The contents of the cecum and large intestine were lavaged similarly using PBS and similarly collected. The cecum and large intestinal wall were saved as one fraction. The stomach contents were emptied by a large incision and subsequent immersion in lavage solution and collected. The stomach wall, liver, and one kidney were collected. All tissue/intestinal content sections were then homogenized in 1 ml of H_2O plus type III protease inhibitor mixture (EMD Biosciences). All samples were then snap-frozen in a dry ice/ethanol bath and stored at −80 °C. Fig. 1*B* depicts visually how we segmented the gastrointestinal tract and other organs for these studies.

Long term feeding studies were carried out by homogeneously mixing purified porcine submaxillary mucin into powdered soy chow at a dose of 100–250 μg of Neu5Gc/g of chow. Chow powder was sterilized prior to feeding. Alternatively, custom chow was prepared professionally (Dyets, Inc.) by mixing mucin into the soy chow ingredients before formulation. We monitored the body weight of the animals to ensure that they thrived equally well on the experimental chows.

Blood and Urine Kinetic Studies—Animals were gavaged, as above. We used the submandibular bleeding technique where blood is sampled from a conscious animal by puncturing the submandibular cheek pouch with a 5.0-mm lancet (Goldenrod Animal Lancets). Minimum blood volume (25–50 μl) was collected in plain glass capillary tubes and allowed to clot in serum microtainers (BD Biosciences). Serum was isolated by spinning tubes at 10,000 rcf for 2 min and stored at −20 °C. Animals were bled at most three times. Urine was collected by restraining a conscious animal and taking advantage of spontaneous urination. If necessary, animals were gently massaged from the sternum in the caudal direction to induce urination. Urine was collected in plain capillary tubes and stored at −80 °C.

Quantification of Free and Glycosidically Linked Neu5Gc by DMB-HPLC—Neu5Gc in tissue, blood, and urine samples was measured by high performance liquid chromatography (HPLC) on a LaChrom Elite HPLC (Hitachi) by tagging sialic acids with the fluorogenic substrate, 1,2-diamino-4,5-methylene-dioxybenzene (DMB, Sigma), using previously described methods (23). HPLC runs were performed at 0.9 ml/min in 85% H_2O, 7% MeOH, 8% CH_3CN. Fluorescent signals were excited at 373 nm and acquired at 448 nm.

Specific volumes of tissue homogenates were taken to maintain total sample sialic acid amounts below a 4-nmol threshold as follows: stomach/small/large intestinal wall samples (100 $\mu l_{homogenate}$); stomach/small/large intestinal contents (100 $\mu l_{homogenate}$); liver (20 $\mu l_{homogenate}$); kidney (20 $\mu l_{homogenate}$); serum (5 $\mu l_{homogenate}$); urine (5 $\mu l_{homogenate}$), and feces (100 $\mu l_{homogenate}$). To quantify free sialic acids in these samples, homogenates were diluted and clarified by centrifugation at 10,000 rcf for 5 min at room temperature. Next, the supernatant was transferred to a Microcon-10, 10,000 molecular weight cutoff centrifugal filter (Millipore) and spun at 14,000 rcf for 15 min. The retentate was washed with 400 μl of H_2O and spun again. Free sialic acids in the run-through were dried down (Eppendorf Vacufuge), resuspended in H_2O, and derivatized with a 2× DMB solution, which contained 7 mM DMB, 1.4 M acetic acid, 0.75 M β-mercaptoethanol, 18 mM sodium hydrosulfite. Samples were derivatized in the dark at 50 °C for 2.5 h. To quantify total sialic acids, sialic acids were first de-*O*-acetylated in 0.1 M NaOH for 30 min at 37 °C. Next, glycosidically linked sialic acids were released by acid hydrolysis in 2 M acetic acid at 80 °C for 3 h. Samples were clarified, spun through a Microcon-10, washed, dried down, resuspended, and derivatized as above. Peak areas on HPLC were quantified by comparison with a standard curve of known Neu5Ac (Inalco Chemicals) and derivatized in parallel. Retention times of Neu5Gc (and Neu5Ac) in a given HPLC experiment were determined using chemically synthesized standards for Neu5Ac and Neu5Gc, as well as known biologic standards for *O*-acetylated sialic acids (purified bovine submaxillary mucin sialic acids), also derivatized in parallel.

Detection of Neu5Gc by Western Blot—Tissue homogenates were lysed by boiling in sample buffer. The supernatant following centrifugation was loaded on 10% polyacrylamide mini gels (Bio-Rad), electrophoresed, and transferred to PVDF mem-

branes (Bio-Rad) using a Fastblot semi-dry transfer system (Biometra). Mild periodate pretreatment of membranes to confirm specificity of anti-Neu5Gc signals was performed by quickly washing PVDF membranes three times in H_2O, washing three times in PBS, pH 6.5, for 5 min, then exposing membranes to freshly made 2 mM $NaIO_4$ in PBS, pH 6.5, for 30 min in the dark at room temperature (or PBS control), then quickly washing membranes three times in H_2O, and finally washing membranes three times in H_2O for 5 min. Blocking, antibody incubations, and washes were then performed on the Snap-ID Vacuum Incubation System (Millipore). Membranes were blocked with 30 ml of 0.5% Neu5Gc-free cold water fish gelatin (Sigma) in Tris-buffered saline containing 0.1% Tween (TBST + FG). Membranes were then incubated with 3 ml of chicken Neu5Gc-specific antibody (αNeu5Gc IgY, Sialix, Inc.), diluted 1:25,000 in TBST, washed six times with 30 ml of TBST + FG, and then incubated with 3 ml of HRP-anti-chicken-IgY (Jackson ImmunoResearch), diluted 1:25,000. Signals were visualized by Immobilon chemiluminescence (Millipore), followed by exposure to Kodak BioMax XAR film for 5–30 s.

Detection of Neu5Gc by Histology—Tissues from animals were either flash-frozen in OCT (Sakura) or fixed in 10% neutral buffered formalin for 24 h and then paraffin-embedded. In the case of the small intestinal segments, each segment was cut open lengthwise and rolled up from the proximal end to the distal end with the mucosal side facing outward. The rolls were fixed in 10% neutral buffered formalin for 24 h, then paraffin-processed, and embedded. The rolls were sectioned at 5 μm, then deparaffinized in xylene, followed by rehydration in graded ethanol dilutions, and submersion in phosphate-buffered saline with 0.1% Tween (PBST). The slides were overlaid with blocking buffer (0.5% cold water fish gelatin in PBST) and blocked for endogenous biotin (Vector Laboratories, Burlingame, CA) and peroxidase. Slides were incubated overnight at 4 °C with the αNeu5Gc IgY (1:5000) and the control IgY (1:5000; Jackson ImmunoResearch). Slides were then washed and incubated with the biotinylated donkey anti-chicken IgY (1:500; Jackson ImmunoResearch) and then with Cy3-streptavidin (1:500; Jackson ImmunoResearch) for 30 min each. Cell nuclei were stained by incubation with DAPI (1:200,000; Sigma). Slides were then mounted in VectaMount (Vector Laboratories) and visualized by fluorescence microscopy.

For cryopreserved liver and postnatal day 1 specimens, frozen sections were cut from the OCT blocks rehydrated in PBST. Next, the slides were blocked for nonspecific binding, blocked for endogenous biotin/peroxidase, and post-fixed in 10% neutral buffered formalin (Fisher). Slides were incubated with antibodies as above, except that the secondary antibody was followed by peroxidase/streptavidin (1:500; Jackson ImmunoResearch), developed with 3-amino-9-ethylcarbazole substrate (Vector Laboratories), and counterstained with Mayer's hematoxylin (Sigma). Slides were then mounted in VectaMount (Vector Laboratories) and visualized by bright field microscopy.

Total Lipid Extraction and Ganglioside Purification—Total lipids were extracted from 200 μl of tissue homogenates using a ratio of 10:10:1 in chloroform/methanol/sample. Samples were vortexed to mix, then bubbled for 30 s with N_2, and sealed. Extraction proceeded at room temperature for 16 h while shaking. Nonlipid materials were pelleted by centrifugation at 2000 rcf for 15 min. Total lipids were then dried down on a Buchler Evapomix and resuspended by sonication (Fisher Sonic Dismembrator) in 1.5 ml of 50 mM KH_2PO_4, pH 7.3. Phospholipids were metabolized by treatment with phospholipase C (Sigma), 5 milliunits/mg_{tissue}, for 6 h at 37 °C. Samples were dried down on a Buchler Evapomix and resuspended in 1 ml of methanol. We used anion exchange chromatography to purify gangliosides (sialoglycolipids) from the remaining neutral lipids. Sephadex A25 resin (GE Healthcare) was swollen in methanol, defined three times with successive washes in methanol, chloroform, 0.8 M sodium acetate (60:30:8) by mixing, and then aspirating the supernatant after the bulk resin had settled. Next, the defined resin was washed three times in methanol/chloroform/water (60:30:8). The activated defined resin was then prepared as a 50% slurry in methanol. Single-use columns were prepared in 5-inch Pasteur pipettes by tamping a small plug of glass wool near the tip, so that the eventual flow rate of the column was ~1 drop/s. Columns were packed with 50% DEAE A25 resin slurry, so that the bed was 3–4 cm in height or an ~1-ml bed volume. Columns were then washed with 6 bed volumes of methanol/chloroform/water (60:30:8) and then with 6 volumes of methanol. 1-ml samples were applied to the column and allowed to run through. The columns were then washed with 6 bed volumes of methanol. Mono-, di-, and trisialogangliosides were eluted together with 6 bed volumes of 0.5 M sodium acetate in methanol. Eluates were dried down and resuspended in 4 ml of methanol/water (1:1). Eluates were desalted using C18 cartridges (Analtech). To desalt, these cartridges were equilibrated with 2 × 10 ml methanol washes, then 2 × 10 ml methanol/water (1:1). Eluates from anion exchange were slowly applied to the cartridge. Cartridges were washed with 4 × 10 ml of water and then eluted with 2 × 10 ml chloroform/methanol (1:1) and 1 × 10 ml chloroform/methanol (2:1). Eluates were dried down. Sialic acids were released from samples by acid hydrolysis and quantified by DMB-HPLC, as described above.

Long Term Neu5Gc-loading Studies—We fed adult $Cmah^{-/-}$ animals continuously with professionally formulated soy chow containing porcine submaxillary mucin (100–250 μg of Neu5Gc/g of chow) *ad libitum*. In addition to fed animals, we also included genotype controls in every experiment (a non-Neu5Gc-fed $Cmah^{-/-}$ mouse and a wild type $Cmah^{+/+}$ mouse). On day 28 of feeding, overnight fasted animals were euthanized and perfused via left ventricular puncture. The lobes of the liver were flipped up to identify hepatic veins, and a minor branching vein off the largest hepatic vein was cut to create an outlet for perfusion. The basic perfusion solution was Krebs-Ringer (122 mM NaCl, 5.6 mM KCl, 5.5 mM D-glucose, 20 mM HEPES, 25 mM $NaHCO_3$, pH adjusted to 7.4, and filter-sterilized). The animals were perfused with 20 ml of warmed Krebs-Ringer solution plus 10 mM EDTA at 7 ml/min. Next, animals were perfused with 20 ml of Krebs-Ringer solution plus 150 μM $CaCl_2$ plus 0.5 mg/ml collagenase type I (from *Clostridium* hemolyticum, Sigma). Target organs (heart, aorta, jejunum, and liver) would lose their red color and become opaque upon collagenase digestion with good perfusion. The organs

TABLE 1

Total recovery of Neu5Gc after feeding free Neu5Gc or Neu5Gc-glycoproteins (glycosidically bound Neu5Gc)

We gavaged equal amounts of Neu5Gc in the form of free Neu5Gc or Neu5Gc-glycoproteins into *Cmah*$^{-/-}$ animals. At the indicated time points, we isolated tissues (stomach, intestines, liver, and blood) and intestinal contents (stomach, small intestine, and large intestine) and quantified the total Neu5Gc that could be recovered as a percentage of the total Neu5Gc fed (0.3 $mmol_{Neu5Gc}$). These recovery values omit any Neu5Gc in the urine (studied separately, see Fig. 1, *E* and *F*) due to the impracticality of consistent urine collection in all mice. No Neu5Gc was detected in fecal material.

Hours after feeding	Hours after feeding	2 h	4 h	6 h
% Neu5Gc recovered	Neu5Gc-glycoprotein fed	60.44 ± 4.8	5.99 ± 2.1	0.40
	Free Neu5Gc fed	18.37	1.50	<0.01

were dissected out of the animal and placed into an iced 6-well plate minced briefly and dissociated using a transfer pipette, and the suspensions were passed through cell strainers (100, 70, 70, and 40 μm, respectively, all from BD Biosciences). The resulting cell suspensions were washed twice in Krebs-Ringer solution plus 150 μM $CaCl_2$ by centrifugation at 300 rcf for 5 min at 4 °C. The final cell pellets were resuspended in 1 ml of Krebs-Ringer solution, and cells were counted on an automated cell counter (Beckman Coulter).

Detection of Cell-surface Neu5Gc by Flow Cytometry—An equal number of cells ($0.1–1.0 \cdot 10^6$ cells depending on the perfusion) were stained for flow cytometry. All cells were stained with αNeu5Gc IgY and with a rat anti-mouse-CD31 (BD Biosciences). All cells were washed by centrifugation and incubated with a donkey anti-chicken-IgY-Cy5 F′ab fragment (Jackson ImmunoResearch) and with a goat anti-mouse-IgG-AlexaFluor488 (Invitrogen). Cells were then washed by centrifugation and resuspended for flow cytometry in PBS. To stain intracellularly for albumin, hepatocytes were stained for Neu5Gc, as above. After staining, cells were fixed and permeabilized according to the Cytofix/Cytoperm kit (BD Biosciences), stained with 1 μg of rabbit anti-albumin (IgG-enriched, Accurate Chemical Co.), and then stained with donkey anti-rabbit-AlexaFluor488 (Invitrogen). Staining was controlled by performing intracellular staining with 1 μg of preimmune rabbit serum as a primary. Cytometry was performed on a BD FACScalibur (BD Biosciences), and the data were analyzed using Flowjo (Treestar).

RESULTS AND DISCUSSION

Ingested Free Neu5Gc Is Only Minimally Recovered from Organs of Fed Mice—We initially compared the total recovery of Neu5Gc from organs of *Cmah*$^{-/-}$ mice at multiple time points following equimolar gavage of free Neu5Gc or Neu5Gc-glycoproteins. As shown in Table 1, the recovery of Neu5Gc (from the entire gastrointestinal tract, the blood, the liver, and the kidneys; excluding urine and feces) was different when comparing the two feeding paradigms. Less than 20% of free Neu5Gc was recovered 2 h after feeding compared with >60% in Neu5Gc-glycoprotein-fed mice. Percentage recoveries drop by a factor of ~10 every 2 h, regardless of feeding paradigm, and Neu5Gc was difficult to recover 4 and 6 h after free Neu5Gc feeding. We hypothesize that the disparity in our recovery of Neu5Gc from free Neu5Gc and Neu5Gc-glycoprotein-fed mice could be due to two factors as follows: (*a*) Neu5Gc might be metabolized by lyases of gut microbial and/or endogenous origin such that we cannot track it using DMB-HPLC, or (*b*) Neu5Gc might be rapidly excreted from the body, as suggested previously (40).

Ingested Free Neu5Gc Is Rapidly Absorbed from the Gastrointestinal Tract and with No Evidence of Metabolic Incorporation into Tissues—To understand the minimal recovery of free Neu5Gc after feeding, we looked for recoveries in multiple individual organs, intestinal contents, blood, and urine. Fig. 1*B* depicts visually how we segmented the gastrointestinal tract and other organs for these studies. Two hours after feeding, Neu5Gc in gastrointestinal (stomach, small, and large intestinal) contents (Fig. 1*C*) of free Neu5Gc-fed mice were markedly lower than in Neu5Gc-glycoprotein-fed mice and also highly variable (10.9 ± 10.1% compared with 45.8 ± 3.8% of total Neu5Gc recovered, respectively). This confirms rapid disappearance of free Neu5Gc from the intestines due to absorption from and/or degradation within the gut. Free Neu5Gc was minimally detected in intestinal wall segments and other tissues (liver, kidney, and blood) (Fig. 1*D*) indicating minimal metabolic incorporation *in vivo*.

Ingested Free Neu5Gc Is Transiently Seen in Blood and Is Efficiently Excreted in Urine—In keeping with the rapid absorption of free Neu5Gc from the intestines, free Neu5Gc levels in blood (Fig. 1*E*, *solid black circles*) peaked 1 h after feeding and quickly declined thereafter. A similar pattern of excretion was seen in urine (Fig. 1*E*, *open gray circles*) with a peak around 30–60 min and minimal amounts by the end of 5 h. These data qualitatively mirror each other and mimic the excretion noted for radioactive free sialic acids (39, 40). The high recovery of free Neu5Gc in urine thus accounts for the poor recovery of Neu5Gc from tissues of free Neu5Gc-fed mice. No Neu5Gc was detected in the feces of free Neu5Gc-fed mice (data not shown). Of the 1 mg of free Neu5Gc that was fed to the animals, we propose that unaccounted for portions are degraded in the gut lumen, perhaps by the microbiome, and/or are metabolized by endogenous metabolic pathways. As our goal was to understand Neu5Gc incorporation into tissues, we did not pursue this matter further.

Fed Neu5Gc-glycoproteins Exhibit Different Intestinal Metabolism, Circulatory Kinetics, and Urine Excretion Compared with Free Neu5Gc—In striking contrast to free Neu5Gc feeding, which was entirely found as a free monosaccharide *in vivo* (intestines/blood/urine), Neu5Gc from Neu5Gc-glycoprotein-fed mice was largely detected on glycans (*e.g.* Neu5Gc glycosidically linked to underlying sugars and presumably a carrier protein/lipid). In tissues and blood, Neu5Gc detection by DMB-HPLC (Fig. 1*E*) required acid hydrolysis for DMB tagging, and in intestines and liver, we were able to track Neu5Gc using αNeu5Gc IgY (Fig. 2). Collectively, these results suggest that dietary Neu5Gc from Neu5Gc-glycoprotein feeding is trafficked *in vivo* in the form of a glycoconjugate.

In Neu5Gc-glycoprotein-fed mice, glycosidically bound Neu5Gc appears in circulation and maintains a near steady state for several hours (Fig. 1*E*, *solid black circles*). Interestingly, Neu5Gc-glycoprotein-fed mice exhibit no excretion of Neu5Gc in urine (Fig. 1*E*, *open gray circles*) up to 48 h after feeding (data

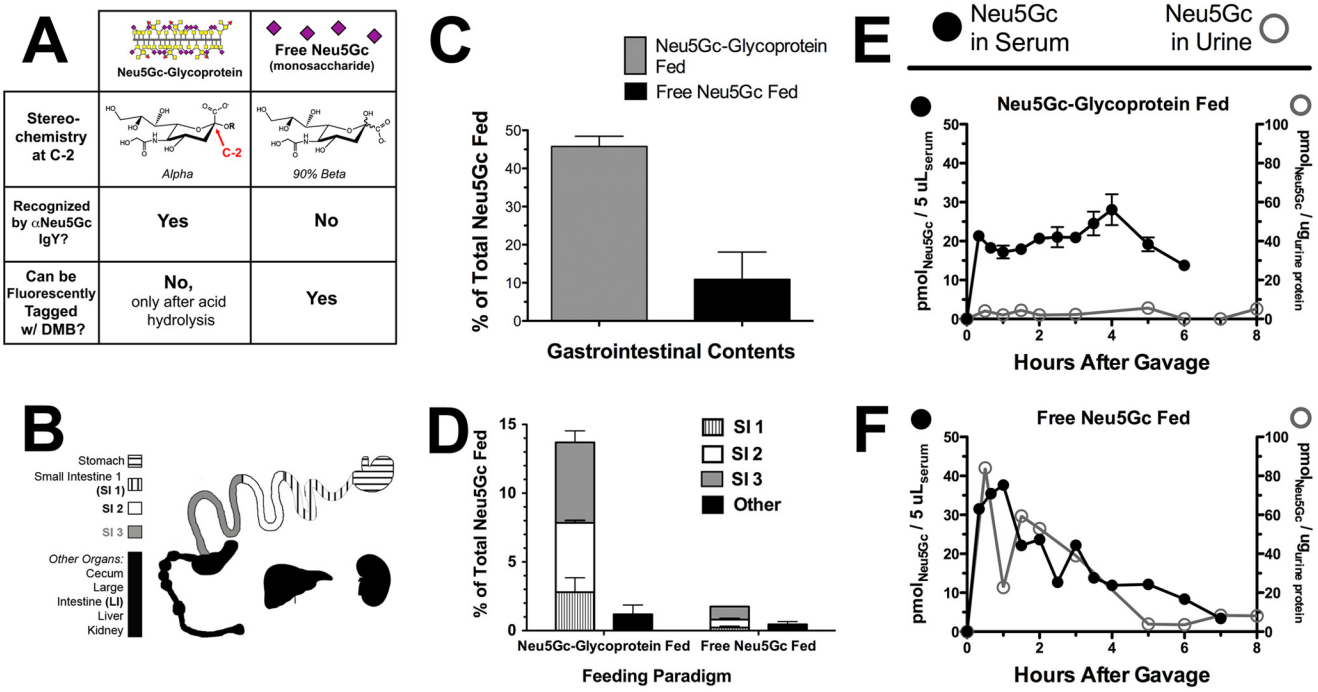

FIGURE 1. **Different gastrointestinal handling of Neu5Gc from free Neu5Gc or Neu5Gc-glycoprotein feeding.** *A,* figure shows the two feeding strategies compared (Neu5Gc-glycoprotein, *left column*; free Neu5Gc, *right column*) and the two key reagents used in this study. αNeu5Gc IgY can recognize glycosidically bound Neu5Gc, such as on PSM ("Neu5Gc-glycoprotein" in this study). DMB is a fluorogenic tag that can react only with free Neu5Gc monosaccharide for quantification in HPLC. Acid hydrolysis can be used to release glycosidically linked Neu5Gc from glycans so that it can be tagged by DMB and is an important process step for quantifying total Neu5Gc (with acid hydrolysis) and free Neu5Gc (without acid hydrolysis). *B,* schematic of tissues studied in this paper. The contents from stomach and small and large intestines were collected. The small intestine was divided into three isometric sections (*SI1*, *SI2*, and *SI3*), along with the samples collected from stomach, large intestine (*LI*), liver, and kidney. Urine and feces were also collected. *C,* Neu5Gc recovered from contents of the gastrointestinal tract (contents from stomach and small and large intestines) was expressed as a percentage of amount gavaged (0.3 mmol of Neu5Gc). We recovered significantly more Neu5Gc from the content of Neu5Gc-glycoprotein-fed mice than free Neu5Gc-fed mice. *D,* marked differences between Neu5Gc recovered from organs of free Neu5Gc and Neu5Gc-glycoprotein-fed mice at 2 h after feeding. SI1 (*hatched bar*), SI2 (*white bar*), SI3 (*gray bar*), and others (*black bar*): liver, kidney, and cecum/LI. Neu5Gc-glycoprotein feeding leads to Neu5Gc being retained in the intestines longer, compared with rapid absorption of free Neu5Gc from the intestinal contents. Neu5Gc from Neu5Gc-glycoprotein feeding is particularly enriched in the terminal small intestine (SI3, *gray bar*). *E, top panel,* blood and urinary excretory kinetics of Neu5Gc in Neu5Gc-glycoprotein-fed mice. Neu5Gc maintains a near steady state for up to 6 h after feeding in blood (*solid black circles*) and is minimally excreted in urine (*open gray circles*) even at the end of 48 h (data not shown). Neu5Gc was very minimally detected in feces from Neu5Gc-glycoprotein-fed mice, ruling it out as major means of excretion. Neu5Gc derived from glycoprotein sources is unlikely to be excreted unchanged in large amounts. *Bottom panel,* free Neu5Gc-fed mice show a spike and rapid disappearance of Neu5Gc from blood (*solid black circles*), indicating that it is rapidly absorbed from the gastrointestinal tract. Neu5Gc in urine from these mice shows similar kinetics, a spike and rapid disappearance (*open gray circles*). The scale of the *y* axes in these panels is the same. Very minimal amounts of free Neu5Gc were detected in feces of free Neu5Gc-fed mice.

not shown). Thus, reduced recovery of Neu5Gc in Neu5Gc-glycoprotein-fed mice at later time points (Table 1) is likely a result of metabolism and not excretion. Two hours after feeding, a high percentage of Neu5Gc can be recovered from the small intestinal walls (Fig. 1*D*). In particular, the terminal part of the small intestine was enriched for Neu5Gc (Fig. 1*D*, *white* and *gray bars*). Detection required acid hydrolysis, indicating the dietary Neu5Gc signal was still glycosidically linked within these small intestinal wall fractions. To be confident that Neu5Gc in the intestinal wall was not due to physical adsorption from gut contents, we also tracked the bacterial octulosonic acid, Kdo, by DMB-HPLC in our intestinal lavage. As >99.5% of Kdo was present in the intestinal content fractions, we reasoned that our intestinal wall fraction was well lavaged, and any Neu5Gc detected here was internalized by the epithelial cells.

We confirmed our HPLC results using αNeu5Gc IgY in immunohistologic analysis of Neu5Gc-glycoprotein-fed intestinal rolls. In Fig. 2*A*, the *top row* shows enriched staining in the middle (*SI2*) and terminal (*SI3*) sections of the small intestine and minimal staining in the proximal small intestine (*SI1*) and large intestine (*LI*), agreeing with our DMB-HPLC analysis. This staining appears within the intestinal villi and does not appear to be associated with the luminal border, but it is rather on the basolateral side of the intestinal enterocytes. To control for this staining, we employed a preimmune chicken IgY (control IgY) on the Neu5Gc-glycoprotein-fed tissues (Fig. 2*A*, *middle row*) and also used αNeu5Gc IgY on non-fed *Cmah*$^{-/-}$ tissues (Fig. 2*A*, *bottom row*), both of which yield no significant staining. To further demonstrate the specificity of our staining, we blocked αNeu5Gc IgY staining with 10% chimpanzee serum (a rich source of Neu5Gc-containing glycans), which abrogated the intestinal staining (Fig. 2*B*). Thus, we conclude that the majority of ingested Neu5Gc-glycoprotein is trafficked through the terminal half of the small intestine, roughly equating to the ileum in humans.

Dietary Neu5Gc-glycoproteins Are Bioavailable for Glycosylation in the Intestines—Feeding Neu5Gc-glycoproteins exhibited drastically different gastrointestinal kinetics than feeding free Neu5Gc, and we reasoned that Neu5Gc-glycoproteins mimic mammalian foods in the human diet more so than a free monosaccharide. Thus, we interpreted that Neu5Gc derived

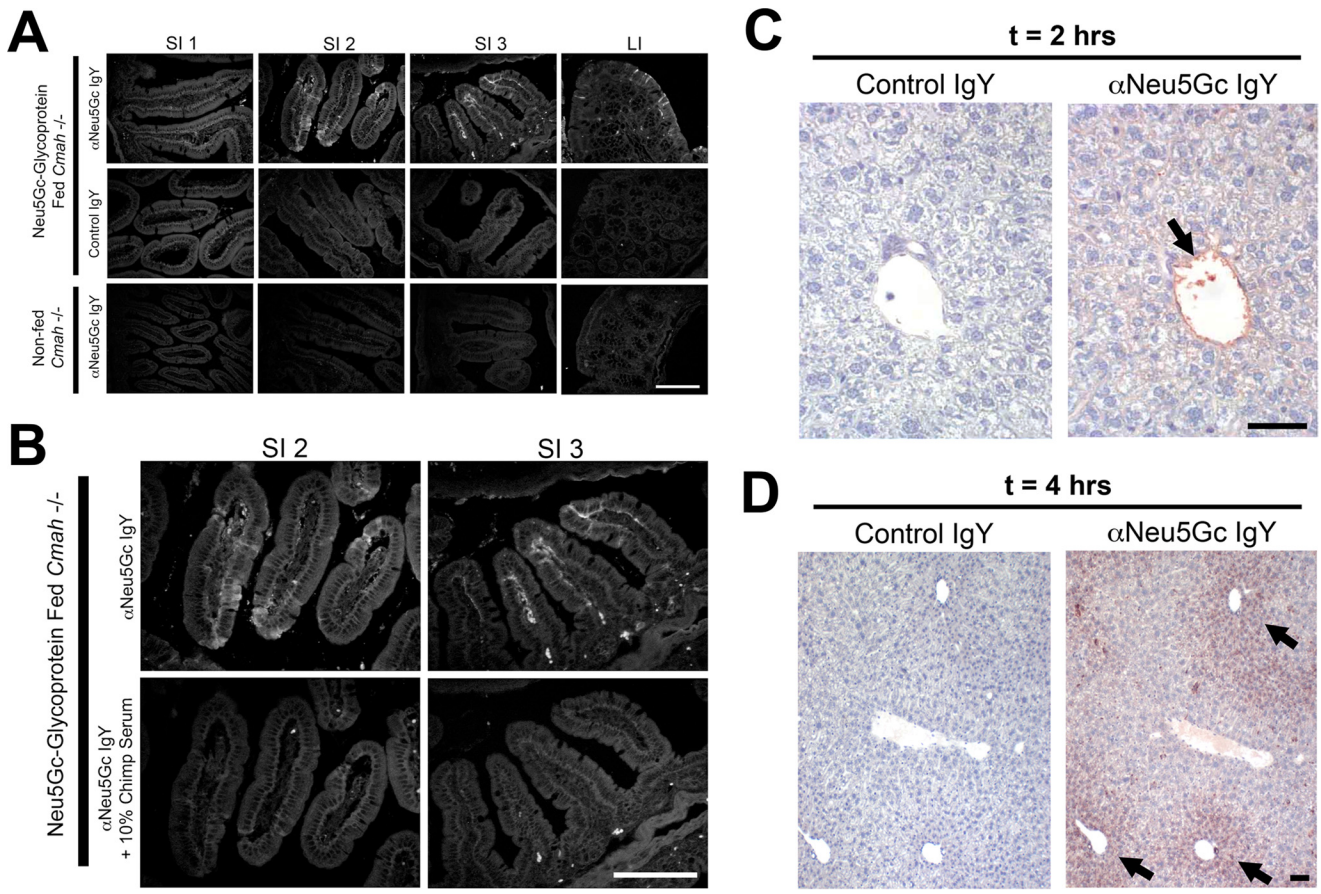

FIGURE 2. **Intestinal uptake of Neu5Gc seen only in Neu5Gc-glycoprotein-fed mice.** *A,* frozen sections of indicated intestine from Neu5Gc-glycoprotein-fed mice 2 h after feeding. Sections are stained with 1:5000 αNeu5Gc IgY (*top row*) showing prominent uptake (*white arrows*) in the middle (*SI2*) and terminal (*SI3)* part of the small intestine, agreeing with Fig. 1*D*. Control IgY shows absence of staining on same tissues (*middle row*). Importantly, tissues from non-fed *Cmah*$^{-/-}$ mice show absence of staining with αNeu5Gc IgY (*bottom row*). *B,* to control for the staining in *A*, we repeated staining in SI2 and SI3 with and without 10% chimpanzee serum during the primary antibody incubation step. Chimpanzee serum is a rich source of Neu5Gc-containing glycoproteins and blocked staining seen by αNeu5Gc IgY in the SI segments (*bottom row*). *C* and *D,* uptake of Neu5Gc in Neu5Gc-glycoprotein-fed mice by the liver. To determine whether Neu5Gc derived from Neu5Gc-glycoprotein feeding is trafficked to peripheral tissues, we harvested livers of fed mice at 2 h (*C*) and 4 h (*D*). Immunohistochemistry using αNeu5Gc IgY revealed staining (*black arrows*) in the portal vein at 2 h (*C*), periportal hepatocytes at 4 h (*D*), and increasingly diffuse periportal hepatocytes at 6 h (figure not shown). *Scale bar,* 100 μm.

from a meal containing Neu5Gc-glycoproteins would be bioavailable for glycosylation, instead of merely being excreted as is the case for dietary free Neu5Gc. The intestines secrete many proteins and lipids that are commonly sialylated, including the apolipoproteins, hormones, and gangliosides (45). Given that glycosylation is occurring in postprandial intestines, we hypothesized that a Neu5Gc-rich meal could contribute to ganglioside synthesis as well as glycoprotein synthesis in the intestine, akin to what happens in cultured cells (18). As the presence of Neu5Gc-containing gangliosides would offer strong evidence for our hypothesis, we used repetitive CH_3Cl/MeOH/sample (10:10:1) extraction of intestinal wall homogenates 2 h after bound Neu5Gc feeding. From the organic fraction, we purified gangliosides and were able to identify Neu5Gc by DMB-HPLC (data not shown), which runs at the same time as a Neu5Gc containing standard.

Notably, the majority of Neu5Gc in this intestinal fraction remained in the protein pellet (data not shown). Control extractions using non-fed intestinal homogenates with exogenous Neu5Gc-GM3 ganglioside added (data not shown) demonstrated the reliability of our methods by recovering Neu5Gc only in the lipid fraction and not in the protein fraction. Control blanks were fractions of non-fed *Cmah*$^{-/-}$ homogenates with no exogenous Neu5Gc-GM3 added, which showed no Neu5Gc peaks.

Importantly, a DMB-HPLC peak that runs at the same time as a Neu5Gc-DMB standard was seen only in samples from PSM-fed animals. Although there were insufficient amounts for accurate mass spectrometric confirmation, we independently confirmed the presence of Neu5Gc by periodate treatment of tissue sections to control for αNeu5Gc IgY binding, as well by using a negative control IgY.

Neu5Gc Derived from Neu5Gc-glycoprotein Feeding Is Bioavailable for Glycosylation in the Liver—To determine whether Neu5Gc from dietary Neu5Gc-glycoproteins can be delivered to peripheral tissues in the *Cmah*$^{-/-}$ mice, we harvested livers at various times for immunohistology with αNeu5Gc IgY, which revealed staining in the portal vein endothelium at 2 h (Fig. 2*C*) and then spread out into the periportal hepatocytes at 4 h (Fig. 2*D*). Western blot analysis of identical samples shows incorporation of Neu5Gc in many endogenous liver glycoproteins (Fig. 3*A*), and the signal increases over time. We controlled for the specificity of αNeu5Gc IgY in Western blots using a mild periodate treatment of the PVDF blotting mem-

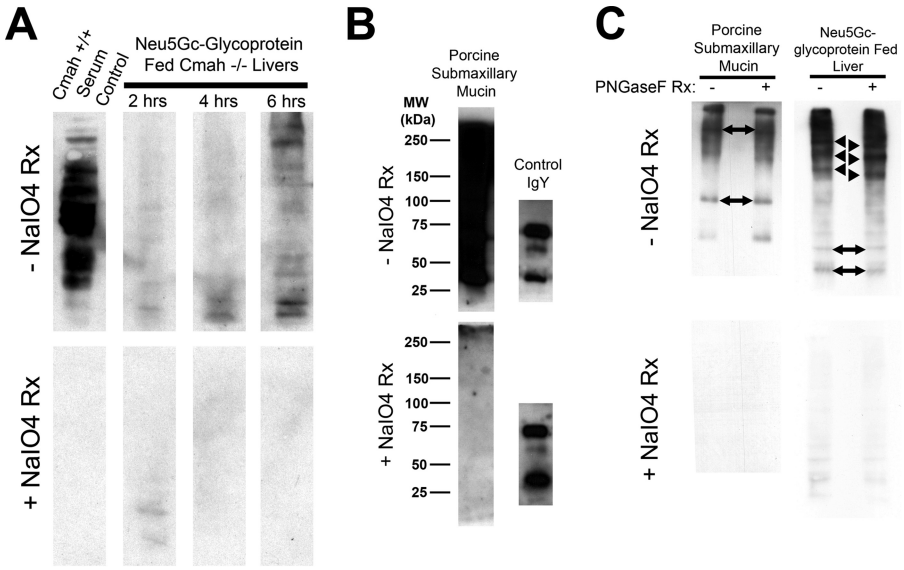

FIGURE 3. **Immunoblots with αNeu5Gc IgY confirm that Neu5Gc from Neu5Gc-glycoprotein feeding is incorporated into endogenous liver glycans.** *A,* immunoblot of Neu5Gc-glycoprotein-fed *Cmah*$^{-/-}$ liver homogenates (25 μg/lane) at the indicated time point with αNeu5Gc IgY with (*bottom*) and without (*top*) periodate treatment (±$NaIO_4$ reaction) of PVDF blotting membrane. Neu5Gc is present on many endogenous liver glycoproteins and signal increases over time. To control for staining, we treated control PVDF membranes with mild periodate (2 mM), which makes Neu5Gc unrecognizable to αNeu5Gc IgY. The positive control, *Cmah*$^{+/+}$ *Serum Control* (*left lane*), is strong, but 100% sensitive to mild periodate treatment (*bottom blot*). *B,* immunoblot of native porcine submaxillary mucin ("Neu5Gc-glycoprotein," 100 ng/lane) with αNeu5Gc IgY, with (*bottom*) and without (*top*) mild periodate treatment (as in *A*). PSM runs as a high molecular weight smear, with no apparent distinct bands. Chicken IgY (100 ng) was included to show that mild periodate treatment does not interfere with epitope recognition of proteins in SDS-PAGE. *C,* immunoblot of Neu5Gc-glycoprotein-fed *Cmah*$^{-/-}$ liver at 6 h with αNeu5Gc IgY with (*bottom*) and without (*top*) periodate treatment. To show that Neu5Gc is bioavailable for endogenous glycan synthesis, we used PNGase-F treatment of liver homogenates. PNGase-F treatment did not remove bands but instead leads to a shift toward a lower apparent molecular weight for several bands (*black arrowhead*) in *+PNGase-F lanes*, compared with *−PNGase-F lanes*. Migration of other bands within the same homogenate was not affected by PNGase-F treatment (*two-sided black arrows*). PSM controls exhibited no apparent shift with PNGase-F treatment, commensurate with mucin-type *O*-GalNAc glycans on PSM (*B*). *Rx* means reaction.

brane, which specifically destroys the C8-C9 side chain of sialic acids (46), a structural feature required for αNeu5Gc IgY binding (see Fig. 3*A*, *column* "*Cmah*$^{+/+}$ *Serum Control*, and data not shown). Note that mild periodate treatment of blotted membranes does not nonspecifically interfere with epitope recognition as conventional protein antigens are still recognized with or without treatment (see "*Control IgY*" *lane* in Fig. 3*B*). Importantly, this staining seen in the livers in Fig. 3*A* is not similar to native PSM run on SDS-PAGE and probed with αNeu5Gc IgY (Fig. 3*B*), indicating that the staining seen in postprandial liver homogenates is not simply due to PSM fragments that have somehow passed through the intestine and reached the liver.

Moreover, Western blots of the liver samples after PNGase-F treatment (Fig. 3*C*) showed a shift in apparent molecular weight of some bands (*black arrowheads*) but not other bands (*two-sided black arrows*). Native PSM control lanes exhibited no shifts or loss of bands upon PNGase-F treatment, indicating that the Neu5Gc-glycoprotein meal was not sensitive to PNGase-F (Fig. 3*C*). Thus, the bands seen in peripheral tissues are not fragments of PSM that have been delivered to these tissues. The fact that PNGase-F treatment did not remove obvious bands in Neu5Gc-glycoprotein-fed liver homogenates, but instead shifted migration behavior in SDS-PAGE, indicates that dietary Neu5Gc had sialylated nascent hepatic *N*-glycan containing glycoproteins soon after a Neu5Gc-rich meal. Taken together, we conclude from these experiments that Neu5Gc is bioavailable for self-glycan synthesis in multiple tissues, within hours of consuming a meal rich in Neu5Gc-glycoprotein.

Although the Neu5Gc in serum and tissues of Neu5Gc-glycoprotein-fed mice was found in glycosidically bound form, the underlying glycoconjugates are currently unknown. The fact that we were able to detect PNGase-F-sensitive Neu5Gc by Western blot of Neu5Gc-GP-fed liver tissues indicates that dietary Neu5Gc does gain access to the overall biosynthetic pool of sialic acids in cell types such as hepatocytes.

Long Term Neu5Gc-glycoprotein Feeding Results in Human-like Incorporation of Neu5Gc in Endothelial and Epithelial Tissues—In keeping with the short term kinetics of free Neu5Gc multiple attempts to load *Cmah*$^{-/-}$ mice with free Neu5Gc monosaccharide failed to recapitulate human-like incorporation in vasculature (21), carcinomas (22), placental tissues (23), or epithelium (25). Our many failed attempts are tabulated in Table 2. They include long term (4–16 weeks) free Neu5Gc in drinking water, which did not yield convincing incorporation by immunohistology with αNeu5Gc IgY, and 4 weeks of bi-weekly intraperitoneal injections of free Neu5Gc, which only leads to minimal incorporation into the tubules of the kidney. In hindsight, the tubule staining result agrees with the finding (Fig. 1*F*) that ingested free Neu5Gc is rapidly excreted into the urine.

We recognized that long term Neu5Gc-glycoprotein feeding is more physiologic and might recapitulate human-like Neu5Gc incorporation. Indeed, immunohistology with αNeu5Gc IgY of 3-week Neu5Gc-glycoprotein-fed mice revealed detectable levels of Neu5Gc incorporation into multiple organs (Fig. 4, *three right columns*). In particular,

TABLE 2
Current and prior attempts at Neu5Gc-loading of *Cmah* null mice
IHC means immunohistochemistry; NA means not applicable.

Loading strategy	Dose	Duration	Detection methods	Comments
		weeks		
$Cmah^{+/-}$ dams carrying $Cmah^{-/-}$ pups	NA	3	HPLC, IHC	$Cmah^{-/-}$ and $Cmah^{+/-}$ born to $Cmah^{-/-}$ sires and $Cmah^{+/-}$ dams. Neu5Gc content of littermate tissues was identical *in utero*
$Cmah^{-/-}$ pups born to $Cmah^{+/-}$ dams	0 (after birth)	NA	HPLC, IHC	$Cmah^{-/-}$ pups born to $Cmah^{+/-}$ dams lost Neu5Gc content rapidly after birth, with levels nearly undetectable at postnatal day 10
$Cmah^{-/-}$ pups born to $Cmah^{-/-}$dams fed Neu5Gc in drinking water	1 mg_{Neu5Gc}/ml	3	IHC	Free Neu5Gc in the drinking water (*ad libitum*) did not load $Cmah^{-/-}$ pups *in utero*[a]
$Cmah^{-/-}$ mice fed Neu5Gc in drinking water long term	1 mg_{Neu5Gc}/ml	10, 16	IHC	Free Neu5Gc in the water (*ad libitum*) led to very weak loading in $Cmah^{-/-}$ mice, and only at very long time points in skeletal muscle, cardiac muscle, and some glands
	1.5 mg_{Neu5Gc}/ml	4	IHC	Mammary tumors from $Cmah^{-/-}$ animals on a spontaneous mammary tumor forming background (MMTV-PyMT transgenic) incorporated Neu5Gc from the drinking water[a]
$Cmah^{-/-}$ mice injected intraperitoneally with free Neu5Gc	40 mg_{Neu5Gc}/kg·day	3	IHC	Animals injected with free Neu5Gc intraperitoneally exhibited loading only of the tubules of the kidney, likely due to excretion into the urine

[a] See Ref. 16.

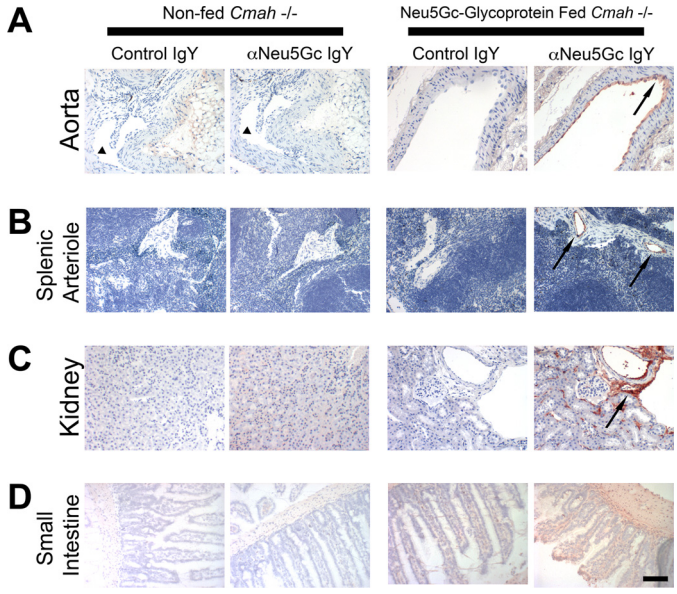

FIGURE 4. **Long term Neu5Gc-glycoprotein feeding leads to metabolic incorporation of Neu5Gc with a human-like tissue distribution I.** *A–D,* paraffin-embedded sections of aorta (*A*), spleen (*B*), kidney (*C*), and small intestine (*D*) of 3-week Neu5Gc-glycoprotein-fed mice were stained with 1:5000 control IgY or αNeu5Gc IgY (*two right columns*). *Brown staining* (see *black arrows*) with αNeu5Gc IgY, which is not seen with Control IgY, indicates that Neu5Gc is incorporated into these tissues. Similar sections from non-fed $Cmah^{-/-}$ tissues were also stained with control IgY or αNeu5Gc IgY (*two left columns*), which showed no staining. Collapsed lumen of non-fed aorta (*A, left columns*) is marked (see *black arrowhead*). *Scale bar,* 100 μm.

vasculature from the aorta (Fig. 4*A*, *black arrow*), spleen (Fig. 4*B*, *black arrow*), and kidney (Fig. 4*C*) showed staining. As expected, the small intestinal villi showed diffuse staining (Fig. 4*D*), indicative of the role of this tissue in dietary trafficking. Importantly, we did not detect Neu5Gc staining in any organs from non-fed $Cmah^{-/-}$ animals (Figs. 2–5, *two left columns*).

At 4 weeks of Neu5Gc-glycoprotein feeding, we analyzed Neu5Gc incorporation by flow cytometry using single cell suspensions from liver, heart, aorta, and small intestine (Fig. 5). These cells (Fig. 5, *red traces*) showed Neu5Gc levels above signals detected when we stained non-fed $Cmah^{-/-}$ cells (*blue traces*). Wild type $Cmah^{+/+}$ cells (Fig. 5, *green traces*) are included for comparison. In fact, cells from aorta, heart, and small intestine of Neu5Gc-glycoprotein-fed mice that were $Neu5Gc^{+}$ largely co-expressed CD31, an endothelial cell marker (Fig. 5*A*). This was not the case in the liver where $Neu5Gc^{+}$ cells were $CD31^{-}$. Subsequent intracellular staining for albumin (a hepatocyte marker) showed that $Neu5Gc^{+}$ events were Alb^{+} (Fig. 5*B*), which agrees with our short term Neu5Gc-glycoprotein feeding immunohistology (Fig. 2*D*), where Neu5Gc was delivered into periportal hepatocytes. Similar assays at 10 weeks of Neu5Gc-glycoprotein feeding showed increased Neu5Gc incorporation in $CD31^{+}$ cells from aorta and from small intestine (Fig. 5*B*), compared with a 4-week feeding. The $CD31^{+}$ pattern of Neu5Gc staining is very similar to that seen in human tissues, supporting the hypothesis that Neu5Gc detected in human tissues is the result of incorporation of dietary Neu5Gc from glycosidically bound, not free sources.

Feeding Neu5Gc-glycoproteins to Pregnant Dams Result in in Utero Incorporation into Fetal Tissues—Past studies reported the presence of Neu5Gc in human fetal meconium (47) and in human fetal tissues and placenta (24). We have previously suspected that the Neu5Gc detected in fetal tissues was the result of incorporation from the maternal diet. However, in prior studies, 1 mg/ml free Neu5Gc in drinking water failed to load fetuses (16). To model a human pregnancy scenario in the mouse, $Cmah^{-/-}$ dams were fed Neu5Gc-glycoprotein chow from fertilization and throughout pregnancy with $Cmah^{-/-}$ pups. Tissue homogenates from postnatal day 1 organs show Neu5Gc incorporation into many glycoproteins, including the small intestine (Fig. 6*A*). Immunohistology of postnatal day 1 animals with αNeu5Gc IgY showed Neu5Gc staining in nearly every tissue examined (Fig. 6*B*), including the cranium and dermis but not the brain itself (Fig. 6*C*). Regarding the lack of brain Neu5Gc, this particular sialic acid is not easily detected in neural tissue of any mammal. This may be explained by our recent studies (48), which suggest that the inability of neural sialidases to cleave α2–8-linked Neu5Gc is the reason why the central nervous system avoids this type of sialic acid. Of course others (32) have shown that dietary Neu5Ac from glycoproteins is traf-

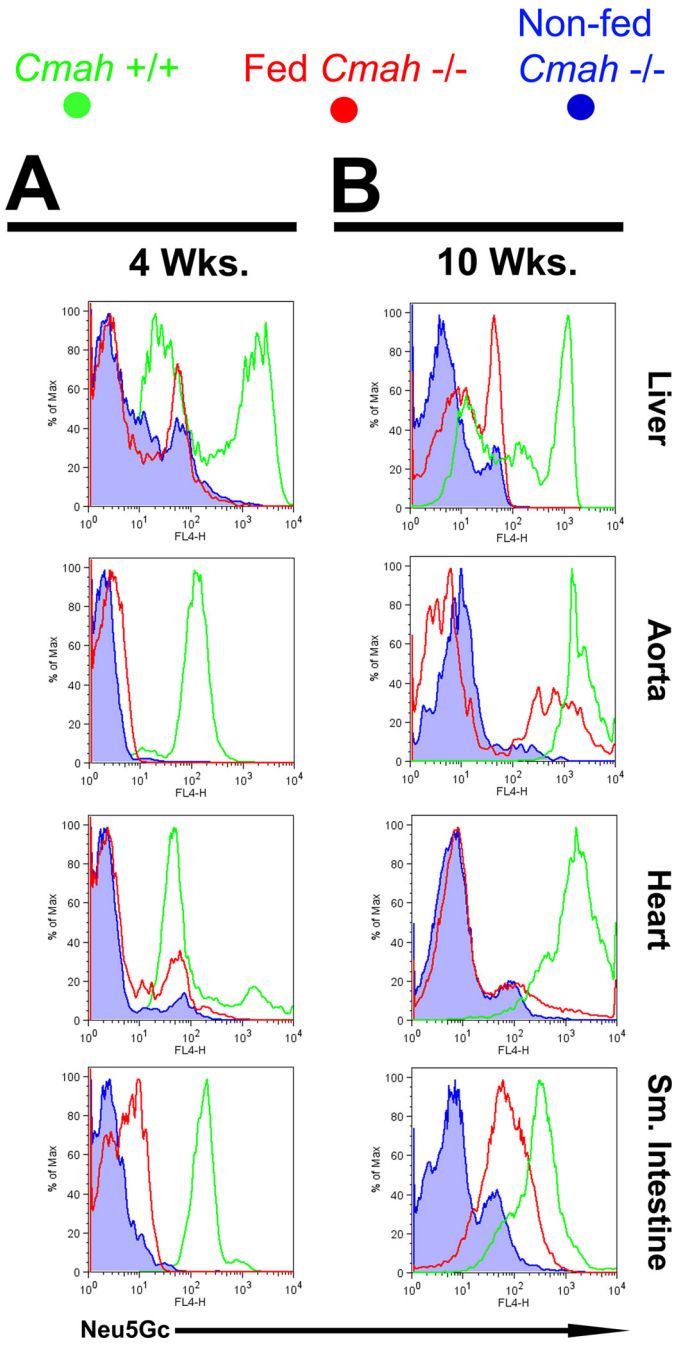

FIGURE 5. **Long term Neu5Gc-glycoprotein feeding leads to metabolic incorporation of Neu5Gc with a human-like tissue distribution II.** *A* and *B*, *Cmah*$^{-/-}$ mice were fed with Neu5Gc-glycoprotein for 3 weeks (*A*) or 10 weeks (*B*). At sacrifice, the animals were perfused with collagenase, and organs were dissociated and stained with αNeu5Gc IgY. Flow cytometric analysis showed positive staining for Neu5Gc in Neu5Gc-glycoprotein-fed mice (*red traces*) above levels seen with non-fed *Cmah*$^{-/-}$ controls (*blue traces*) at 4 weeks of feeding (*A*) and increased further at 10 weeks of feeding (*B*). Most Neu5Gc-positive events from heart, aorta, and small intestine co-stained with a marker for endothelium (CD31), although Neu5Gc-positive events in the liver co-stained with a marker for hepatocytes (albumin). Tissues from *Cmah*$^{+/+}$ mice were used as positive controls and for comparison (*green traces*). These results are representative results from Neu5Gc feeding courses that were repeated at least three times on *Cmah*$^{-/-}$ animals, staining three Neu5Gc-glycoprotein-fed mice per feeding time point.

ficked into the brain during rapid central nervous system development. It may be that the developing nervous system requirement for sialic acid underlies the specific mechanism for the fetal Neu5Gc uptake from the mother that we describe here. The fact that brain incorporation does not happen to Neu5Gc suggests that this organ has additional mechanisms to exclude or destroy any Neu5Gc that arrives from external sources.

Cmah$^{-/-}$ pups were maintained on a Neu5Gc-glycoprotein chow after weaning and studied 4 weeks after birth by immunohistology with αNeu5Gc IgY. These animals showed similar patterns of staining, indicating that Neu5Gc was still accumulating through the diet after birth. Neu5Gc staining was not restricted to endothelial and epithelial tissues in pre-natal/post-natal loaded *Cmah*$^{-/-}$ mice, and we could detect Neu5Gc at sites like smooth muscle bundles (data not shown), skeletal muscle fibers (data not shown), and in the endocardium (Fig. 6*B*), patterns not yet seen in human tissues. Throughout our experiments, we have seen a consistent and selective enrichment for Neu5Gc incorporation in endothelial and epithelial cells and not in some other cells types. Understanding the delivery mechanism by which dietary Neu5Gc is trafficked through the bloodstream may explain these patterns. This will be the subject of future studies.

Neu5Gc-glycoprotein Feeding Results in Incorporation into Developing Tumors—The presence of Neu5Gc in human carcinomas has been reported several times, and Neu5Gc was previously hypothesized to be an oncofetal antigen in human cancer (47). However, human carcinoma cells that are cultured in Neu5Gc-free media become Neu5Gc-free over time (18), and oncogene-induced breast carcinomas in *Cmah*$^{-/-}$ mice were Neu5Gc-free, until free Neu5Gc feeding in the drinking water at 1.5 mg of Neu5Gc/ml over 4 weeks yielded weak incorporation in the tumors (16).

We hypothesized that we could load tumors *in vivo* with Neu5Gc-glycoproteins. We injected 10^6 syngeneic MC38 carcinoma cells subcutaneously into the flanks of *Cmah*$^{-/-}$ mice. The mice were then split into three groups as follows: 1) maintained on Neu5Gc-free soy chow; 2) moved to free Neu5Gc in the drinking water; 3) moved to Neu5Gc-glycoprotein chow. Tumor growth was not statistically different between the groups over the 3-week course (data not shown). We used our flow cytometry-based assay to detect Neu5Gc levels on MC38 cells isolated from the flank tumor. Similar to previous results with free Neu5Gc feeding and cancer (16), free Neu5Gc feeding in this model led to increased Neu5Gc incorporation above base line in MC38 cells compared with tumor cells grown in animals on the Neu5Gc-free soy chow (Fig. 7, *left panel, black trace*). However, MC38 cells from Neu5Gc-glycoprotein-fed mice exhibited substantially more Neu5Gc incorporation compared with both free Neu5Gc-fed and soy chow-fed mouse tumor cells (Fig. 7, *right panel, black trace*). It was interesting that Neu5Gc-glycoprotein feeding did not led to increased intensity of staining, compared with free Neu5Gc feeding, but instead led to a larger proportion of cells being Neu5Gc-positive. This result indicates that both free Neu5Gc and Neu5Gc-glycoprotein feeding can load developing tumors, but Neu5Gc-glycoprotein feeding gains access to a greater proportion of the tumor. This is likely due to the poorly understood delivery mechanism of Neu5Gc-glycoprotein to peripheral tissues.

Once again, tumorigenesis was the only scenario where free Neu5Gc feeding resulted in some detectable Neu5Gc incorpo-

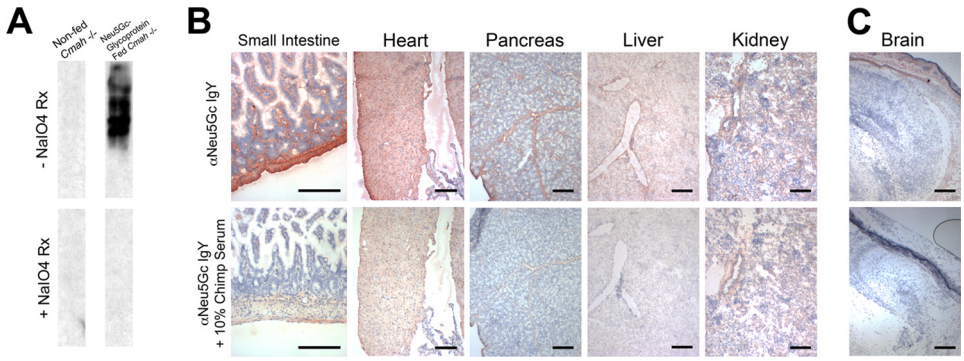

FIGURE 6. **Maternal dietary Neu5Gc is metabolically incorporated *in utero* in newborn tissues.** *A,* Western blot analysis with αNeu5Gc IgY demonstrates Neu5Gc on multiple glycoproteins of fetal small intestinal homogenates (*top*) that is sensitive to periodate treatment (+$NaIO_4$ reaction, *bottom*). *B,* immunohistochemistry with αNeu5Gc IgY of multiple tissues from *in utero* loaded *Cmah*$^{-/-}$ newborns indicated widespread incorporation of dietary Neu5Gc, in patterns that exceed those seen with adult feeding. *In utero* loaded mice demonstrate staining with αNeu5Gc IgY many tissues, including heart, smooth muscle (surrounding intestinal villi), pancreas, liver, and kidney (*top row*). Staining was controlled with 10% chimpanzee serum block (*bottom row*). *C,* consistent with the human condition, we were still unable to load Neu5Gc into the brain, although the cranial and dermis tissue surrounding the brain show staining with αNeu5Gc IgY (*top row*) that is sensitive to block with chimpanzee serum (*bottom row*). *Scale bar,* 100 μm.

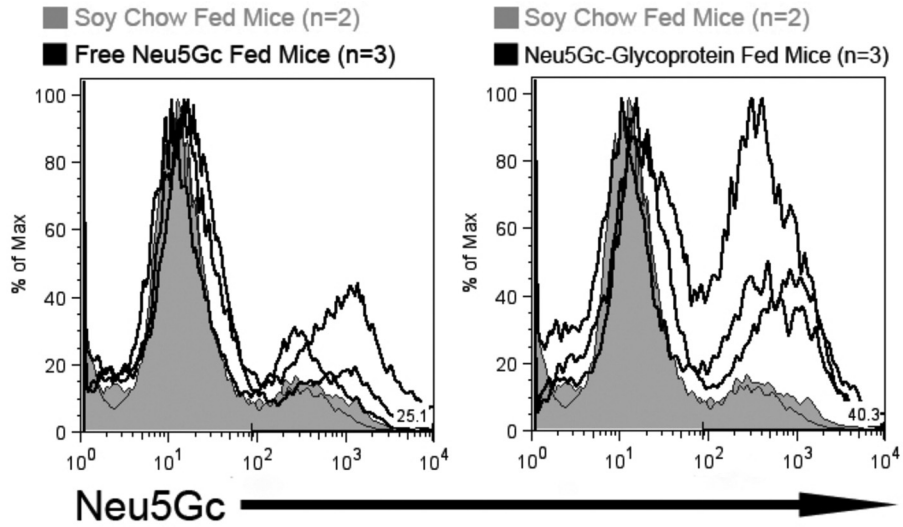

FIGURE 7. **Dietary Neu5Gc is incorporated in growing tumors *in vivo*.** To determine whether dietary Neu5Gc can be incorporated in tumors *in vivo*, adult *Cmah*$^{-/-}$ mice were injected subcutaneously with $0.5 \cdot 10^6$ MC38 cells and fed no Neu5Gc (soy chow fed, *tinted gray histograms*, $n = 2$), fed free Neu5Gc (*solid line* in the *left histogram*, $n = 3$), or fed glycosidically bound Neu5Gc (*solid line* in *right histogram*, $n = 3$) for 3 weeks. Tumors were removed and digested into single cell suspensions using collagenase. 10^6 tumor cells from each mouse were stained αNeu5Gc IgY for flow cytometric analysis. Neu5Gc was incorporated into tumor cells from Neu5Gc-glycoprotein-fed mice and free Neu5Gc-fed mice, although at lower levels as indicated by the lower intensity of staining.

ration *in vivo*. If reliable in humans, this observation could be exploited to deliberately load tumors. Because ingested free Neu5Gc is poorly incorporated into normal tissues, tumor cells could be selectively labeled. Introduction of a Neu5Gc-specific toxin or inflammation associated with recognition by the human Neu5Gc-specific antibody response could then target the tumor for cytologic or immunologic attack, respectively. Regardless of these speculations, the "oncofetal" prominence of Neu5Gc in humans can likely be attributed to metabolic incorporation of Neu5Gc-glycoproteins from the diet.

Conclusions and Perspectives—We have previously found trace amounts of Neu5Gc in a characteristic incorporation pattern in normal human tissues (24), despite the fact that humans are genetically unable to produce Neu5Gc. The cells types in question are endothelium of small and large blood vessels, intestinal epithelium (epithelium lining hollow organs), placenta, fetal tissues, and some carcinomas. We hypothesized that Neu5Gc in human tissues is metabolically incorporated from the diet. However, many failed experiments in the mouse (Table 2) indicated that the mere presence of free Neu5Gc *in vivo* was not sufficient to achieve this. The current data have expanded upon a metabolic pathway for dietary incorporation of sialic acids shown previously (39, 40) and have significantly deepened these observations by showing for the first time that dietary Neu5Gc-containing glycoproteins are metabolically incorporated *in vivo* in a human-like tissue distribution (Figs. 4 and 5). The striking contrast of Neu5Gc-glycoprotein feeding with the negative results of free Neu5Gc feeding (Fig. 1) indicates that there exists a novel pathway for intestinal processing of glycosidically bound Neu5Gc, with subsequent delivery and incorporation into peripheral tissues. Free Neu5Gc is rapidly absorbed from the intestines and appears rapidly in blood, only to end up in urine in short term feeding studies. Long term loading studies agree that free Neu5Gc feeding does not work (Table 2). However, Neu5Gc-glycoprotein feeding exhibits different handling in the small intestine and throughout the body,

disappearing more slowly from the intestine and with persistence in the blood and in the liver. Further studies are needed to elucidate the transport mechanism underlying this pathway.

The PSM polypeptide is serine-rich, highly polymorphic, and heavily glycosylated with *O*-glycans (49, 50). Because the human diet contains a mixture of *N*- and *O*-linked glycoproteins, as well as glycolipids and oligosaccharides, the question remains whether the structure of the underlying glycan changes Neu5Gc uptake and trafficking. Further studies are needed to clarify and understand any significant differences among classes of Neu5Gc-bearing glycoconjugates and/or types of food sources.

We also cannot be certain if the α/β anomeric configuration differences between free Neu5Gc and Neu5Gc-glycoproteins contributes to the differences shown in this study. Early dietary studies of fed oligosaccharides (39, 40) appeared to show similar metabolic and excretory kinetics as free Neu5Gc in our studies. Based on all the data, it is reasonable to speculate that the same may be true with other smaller Neu5Gc-sialoglycans. Studies of postprandial serum from Neu5Gc-GP-fed mice are also needed to shed light on the transport mechanism of dietary Neu5Gc from the gut to the peripheral tissues.

Other aspects of underlying mechanisms need further exploration. Although we have not shown it here *in vivo*, our previous studies (18) demonstrated *in vitro* that Neu5Gc-glycoproteins can be taken up by macropinocytosis and processed in the lysosome to release free Neu5Gc, which is then transported to the cytosol by the lysosomal sialic acid exporter, for reuse in sialylation. It is possible that dietary Neu5Gc is exploiting some facet of this salvage pathway.

Regardless, it seems unlikely that humans and mice have evolved this system purely to scavenge dietary Neu5Gc (indeed, the typical diet of a wild mouse in unlikely to contain much mammalian-derived Neu5Gc). Given the striking differences in kinetics of free Neu5Gc and Neu5Gc-glycoprotein meals, the ability of Neu5Gc-glycoproteins to result in metabolic incorporation in specific tissues, and the apparent need for dietary sialic acids at critical periods of mammalian growth (32–34), it is likely that we are actually studying a general pathway for incorporation of dietary sialic acids. The bloodstream transport molecule(s) for Neu5Gc needs to be studied to better understand the *in vivo* transport mechanism for dietary Neu5Gc. This will shed light on the heretofore unexplained pattern of dietary Neu5Gc tissue incorporation seen in humans and now in *Cmah*$^{-/-}$ mice. However, the ability of free Neu5Gc to load subcutaneous carcinomas (Fig. 7) presents an interesting possibility of selectively incorporating Neu5Gc into tumors for therapeutic reasons. While pursuing this tumor-labeling strategy, it will be important to ensure that free Neu5Gc does not load physiologic tissues *in vivo*, even at low levels.

In conclusion, we are beginning to understand how humans metabolically incorporate dietary Neu5Gc. This information has important ramifications for human health and underscores the importance of minimizing dietary intake of Neu5Gc, presumably to reduce the body burden of Neu5Gc (although we have little data regarding the turnover of incorporated Neu5Gc in humans). Reducing dietary Neu5Gc should also limit the risk for Neu5Gc-binding Shiga-like toxins (25) as well as minimize the interaction of Neu5Gc-specific antibodies and incorporated Neu5Gc in promoting vasculitis (21) or carcinoma progression (22).

Acknowledgments—We thank Sandra Diaz and Michelle Chung for comments and for help with some of the experiments.

REFERENCES

1. Schauer, R. (1978) Characterization of sialic acids. *Methods Enzymol.* **50,** 64–89
2. Troy, F. A. (1992) Polysialylation. From bacteria to brains. *Glycobiology* **2,** 5–23
3. Varki, A., and Schauer, R. (2009) in *Essentials of Glycobiology* (Varki, A., Cummings, R. D., Esko, J. D., Freeze, H. H., Stanley, P., Bertozzi, C. R., Hart, G. W., and Etzler, M. E., eds) pp. 199–218, Cold Spring Harbor Laboratory Press, Cold Spring Harbor, NY
4. Schwarzkopf, M., Knobeloch, K. P., Rohde, E., Hinderlich, S., Wiechens, N., Lucka, L., Horak, I., Reutter, W., and Horstkorte, R. (2002) Sialylation is essential for early development in mice. *Proc. Natl. Acad. Sci. U.S.A.* **99,** 5267–5270
5. Shaw, L., and Schauer, R. (1988) The biosynthesis of *N*-glycoloylneuraminic acid occurs by hydroxylation of the CMP-glycoside of *N*-acetylneuraminic acid. *Biol. Chem. Hoppe-Seyler* **369,** 477–486
6. Shaw, L., Schneckenburger, P., Schlenzka, W., Carlsen, J., Christiansen, K., Jürgensen, D., and Schauer, R. (1994) CMP-*N*-acetylneuraminic acid hydroxylase from mouse liver and pig submandibular glands. Interaction with membrane-bound and soluble cytochrome b_5-dependent electron transport chains. *Eur. J. Biochem.* **219,** 1001–1011
7. Takematsu, H., Kawano, T., Koyama, S., Kozutsumi, Y., Suzuki, A., and Kawasaki, T. (1994) Reaction mechanism underlying CMP-*N*-acetylneuraminic acid hydroxylation in mouse liver. Formation of a ternary complex of cytochrome b_5, CMP-*N*-acetylneuraminic acid, and a hydroxylation enzyme. *J. Biochem.* **115,** 381–386
8. Kawano, T., Koyama, S., Takematsu, H., Kozutsumi, Y., Kawasaki, H., Kawashima, S., Kawasaki, T., and Suzuki, A. (1995) Molecular cloning of cytidine monophospho-*N*-acetylneuraminic acid hydroxylase. Regulation of species- and tissue-specific expression of *N*-glycolylneuraminic acid. *J. Biol. Chem.* **270,** 16458–16463
9. Kelm, S., and Schauer, R. (1997) Sialic acids in molecular and cellular interactions. *Int. Rev. Cytol.* **175,** 137–240
10. Angata, T., and Varki, A. (2002) Chemical diversity in the sialic acids and related α-keto acids. An evolutionary perspective. *Chem. Rev.* **102,** 439–469
11. Varki, A. (2010) Colloquium paper. Uniquely human evolution of sialic acid genetics and biology. *Proc. Natl. Acad. Sci. U.S.A.* **107,** 8939–8946
12. Bergfeld, A. K., Pearce, O. M., Diaz, S. L., Pham, T., and Varki, A. (2012) Metabolism of vertebrate amino sugars with *N*-glycolyl groups. Elucidating the intracellular fate of the non-human sialic acid *N*-glycolylneuraminic acid. *J. Biol. Chem.* **287,** 28865–28881
13. Irie, A., Koyama, S., Kozutsumi, Y., Kawasaki, T., and Suzuki, A. (1998) The molecular basis for the absence of *N*-glycolylneuraminic acid in humans. *J. Biol. Chem.* **273,** 15866–15871
14. Chou, H. H., Takematsu, H., Diaz, S., Iber, J., Nickerson, E., Wright, K. L., Muchmore, E. A., Nelson, D. L., Warren, S. T., and Varki, A. (1998) A mutation in human CMP-sialic acid hydroxylase occurred after the Homo-Pan divergence. *Proc. Natl. Acad. Sci. U.S.A.* **95,** 11751–11756
15. Hayakawa, T., Satta, Y., Gagneux, P., Varki, A., and Takahata, N. (2001) Alu-mediated inactivation of the human CMP-*N*-acetylneuraminic acid hydroxylase gene. *Proc. Natl. Acad. Sci. U.S.A.* **98,** 11399–11404
16. Hedlund, M., Tangvoranuntakul, P., Takematsu, H., Long, J. M., Housley, G. D., Kozutsumi, Y., Suzuki, A., Wynshaw-Boris, A., Ryan, A. F., Gallo, R. L., Varki, N., and Varki, A. (2007) *N*-Glycolylneuraminic acid deficiency in mice. Implications for human biology and evolution. *Mol. Cell. Biol.* **27,** 4340–4346
17. Naito, Y., Takematsu, H., Koyama, S., Miyake, S., Yamamoto, H., Fujinawa, R., Sugai, M., Okuno, Y., Tsujimoto, G., Yamaji, T., Hashimoto, Y.,

Itohara, S., Kawasaki, T., Suzuki, A., and Kozutsumi, Y. (2007) Germinal center marker GL7 probes activation-dependent repression of *N*-glycolylneuraminic acid, a sialic acid species involved in the negative modulation of B-cell activation. *Mol. Cell. Biol.* **27,** 3008–3022
18. Bardor, M., Nguyen, D. H., Diaz, S., and Varki, A. (2005) Mechanism of uptake and incorporation of the non-human sialic acid *N*-glycolylneuraminic acid into human cells. *J. Biol. Chem.* **280,** 4228–4237
19. Malykh, Y. N., Schauer, R., and Shaw, L. (2001) *N*-Glycolylneuraminic acid in human tumors. *Biochimie* **83,** 623–634
20. Schauer, R., Srinivasan, G. V., Coddeville, B., Zanetta, J. P., and Guérardel, Y. (2009) Low incidence of *N*-glycolylneuraminic acid in birds and reptiles and its absence in the platypus. *Carbohydr. Res.* **344,** 1494–1500
21. Pham, T., Gregg, C. J., Karp, F., Chow, R., Padler-Karavani, V., Cao, H., Chen, X., Witztum, J. L., Varki, N. M., and Varki, A. (2009) Evidence for a novel human-specific xeno-autoantibody response against vascular endothelium. *Blood* **114,** 5225–5235
22. Hedlund, M., Padler-Karavani, V., Varki, N. M., and Varki, A. (2008) Evidence for a human-specific mechanism for diet and antibody-mediated inflammation in carcinoma progression. *Proc. Natl. Acad. Sci. U.S.A.* **105,** 18936–18941
23. Diaz, S. L., Padler-Karavani, V., Ghaderi, D., Hurtado-Ziola, N., Yu, H., Chen, X., Brinkman-Van der Linden, E. C., Varki, A., and Varki, N. M. (2009) Sensitive and specific detection of the non-human sialic acid *N*-glycolylneuraminic acid in human tissues and biotherapeutic products. *PLoS ONE* **4,** e4241
24. Tangvoranuntakul, P., Gagneux, P., Diaz, S., Bardor, M., Varki, N., Varki, A., and Muchmore, E. (2003) Human uptake and incorporation of an immunogenic nonhuman dietary sialic acid. *Proc. Natl. Acad. Sci. U.S.A.* **100,** 12045–12050
25. Byres, E., Paton, A. W., Paton, J. C., Löfling, J. C., Smith, D. F., Wilce, M. C., Talbot, U. M., Chong, D. C., Yu, H., Huang, S., Chen, X., Varki, N. M., Varki, A., Rossjohn, J., and Beddoe, T. (2008) Incorporation of a non-human glycan mediates human susceptibility to a bacterial toxin. *Nature* **456,** 648–652
26. Nguyen, D. H., Tangvoranuntakul, P., and Varki, A. (2005) Effects of natural human antibodies against a non-human sialic acid that metabolically incorporates into activated and malignant immune cells. *J. Immunol.* **175,** 228–236
27. Padler-Karavani, V., Yu, H., Cao, H., Chokhawala, H., Karp, F., Varki, N., Chen, X., and Varki, A. (2008) Diversity in specificity, abundance, and composition of anti-Neu5Gc antibodies in normal humans. Potential implications for disease. *Glycobiology* **18,** 818–830
28. Padler-Karavani, V., Hurtado-Ziola, N., Pu, M., Yu, H., Huang, S., Muthana, S., Chokhawala, H. A., Cao, H., Secrest, P., Friedmann-Morvinski, D., Singer, O., Ghaderi, D., Verma, I. M., Liu, Y. T., Messer, K., Chen, X., Varki, A., and Schwab, R. (2011) Human xeno-autoantibodies against a non-human sialic acid serve as novel serum biomarkers and immunotherapeutics in cancer. *Cancer Res.* **71,** 3352–3363
29. Taylor, R. E., Gregg, C. J., Padler-Karavani, V., Ghaderi, D., Yu, H., Huang, S., Sorensen, R. U., Chen, X., Inostroza, J., Nizet, V., and Varki, A. (2010) Novel mechanism for the generation of human xeno-autoantibodies against the nonhuman sialic acid *N*-glycolylneuraminic acid. *J. Exp. Med.* **207,** 1637–1646
30. Yin, J., Hashimoto, A., Izawa, M., Miyazaki, K., Chen, G. Y., Takematsu, H., Kozutsumi, Y., Suzuki, A., Furuhata, K., Cheng, F. L., Lin, C. H., Sato, C., Kitajima, K., and Kannagi, R. (2006) Hypoxic culture induces expression of sialin, a sialic acid transporter, and cancer-associated gangliosides containing non-human sialic acid on human cancer cells. *Cancer Res.* **66,** 2937–2945
31. Löfling, J. C., Paton, A. W., Varki, N. M., Paton, J. C., and Varki, A. (2009) A dietary non-human sialic acid may facilitate hemolytic-uremic syndrome. *Kidney Int.* **76,** 140–144
32. Wang, B. (2009) Sialic acid is an essential nutrient for brain development and cognition. *Annu. Rev. Nutr.* **29,** 177–222
33. Wang, B., Yu, B., Karim, M., Hu, H., Sun, Y., McGreevy, P., Petocz, P., Held, S., and Brand-Miller, J. (2007) Dietary sialic acid supplementation improves learning and memory in piglets. *Am. J. Clin. Nutr.* **85,** 561–569
34. Bode, L. (2009) Human milk oligosaccharides. Prebiotics and beyond. *Nutr. Rev.* **67,** S183–S191
35. Wang, B., Brand-Miller, J., McVeagh, P., and Petocz, P. (2001) Concentration and distribution of sialic acid in human milk and infant formulas. *Am. J. Clin. Nutr.* **74,** 510–515
36. Morgan, B. L., and Winick, M. (1979) A possible relationship between brain *N*-acetylneuraminic acid content and behavior. *Proc. Soc. Exp. Biol. Med.* **161,** 534–537
37. Anderson, J. W., Johnstone, B. M., and Remley, D. T. (1999) Breast-feeding and cognitive development. A meta-analysis. *Am. J. Clin. Nutr.* **70,** 525–535
38. Dickson, J. J., and Messer, M. (1978) Intestinal neuraminidase activity of suckling rats and other mammals. Relationship to the sialic acid content of milk. *Biochem. J.* **170,** 407–413
39. Nöhle, U., Beau, J. M., and Schauer, R. (1982) Uptake, metabolism, and excretion of orally and intravenously administered, double-labeled *N*-glycoloylneuraminic acid and single-labeled 2-deoxy-2,3-dehydro-*N*-acetylneuraminic acid in mouse and rat. *Eur. J. Biochem.* **126,** 543–548
40. Nöhle, U., and Schauer, R. (1981) Uptake, metabolism, and excretion of orally and intravenously administered, ^{14}C- and ^{3}H-labeled *N*-acetylneuraminic acid mixture in the mouse and rat. *Hoppe-Seyler's Z. Physiol. Chem.* **362,** 1495–1506
41. Nöhle, U., and Schauer, R. (1984) Metabolism of sialic acids from exogenously administered sialyllactose and mucin in mouse and rat. *Hoppe-Seyler's Z. Physiol. Chem.* **365,** 1457–1467
42. Varki, A., and Diaz, S. (1984) The release and purification of sialic acids from glycoconjugates. Methods to minimize the loss and migration of *O*-acetyl groups. *Anal. Biochem.* **137,** 236–247
43. Pearce, O. M., and Varki, A. (2010) Chemo-enzymatic synthesis of the carbohydrate antigen *N*-glycolylneuraminic acid from glucose. *Carbohydr. Res.* **345,** 1225–1229
44. Gottschalk, A. (1960) *The Chemistry and Biology of Sialic Acids and Related Substances*, pp. 1–115, Cambridge University Press, Cambridge, UK
45. Tso, P., and Balint, J. A. (1986) Formation and transport of chylomicrons by enterocytes to the lymphatics. *Am. J. Physiol.* **250,** G715–G26
46. Norgard, K. E., Han, H., Powell, L., Kriegler, M., Varki, A., and Varki, N. M. (1993) Enhanced interaction of L-selectin with the high endothelial venule ligand via selectively oxidized sialic acids. *Proc. Natl. Acad. Sci. U.S.A.* **90,** 1068–1072
47. Hirabayashi, Y., Kasakura, H., Matsumoto, M., Higashi, H., Kato, S., Kasai, N., and Naiki, M. (1987) Specific expression of unusual GM2 ganglioside with Hanganutziu-Deicher antigen activity on human colon cancers. *Jpn. J. Cancer Res.* **78,** 251–260
48. Davies, L., Pearce, O. M., Tessier, M., Assar, S., Smutova, V., Pajunen, M., Sumida, M., Sato, C., Kitajima, K., Finne, J., Gagneux, P., Pchejetsky, A., Woods, R., and Varki, A. (2012) Metabolism of vertebrate amino sugars with *N*-glycolyl groups. Resistance of α2–8-linked *N*-glycolylneuraminic acid to enzymatic cleavage. *J. Biol. Chem.* **287,** 28917–28931
49. Carlson, D. M. (1968) Structures and immunochemical properties of oligosaccharides isolated from pig submaxillary mucins. *J. Biol. Chem.* **243,** 616–626
50. Eckhardt, A. E., Timpte, C. S., DeLuca, A. W., and Hill, R. L. (1997) The complete cDNA sequence and structural polymorphism of the polypeptide chain of porcine submaxillary mucin. *J. Biol. Chem.* **272,** 33204–33210